



Comparison of the mechanical performance of concrete reinforced with recycled steel fibers from waste tires and hooked-end steel fibers at ambient and high temperatures

Yaghout Modarres¹ and Mansour Ghalehnovi^{2*}

¹ Ph.D. Candidate, Department of Civil Engineering, Ferdowsi University of Mashhad, Mashhad, Iran.

² Professor, Department of Civil Engineering, Ferdowsi University of Mashhad, Mashhad, Iran.

Received: 11/10/2022

Revised: 15/04/2023

Accepted: 12/06/2023

Abstract

In this experimental study, a mechanical and economic analysis has been done to investigate the performance of recycled steel fibers (RSF) from waste tires. Two types of recycled fibers, including recycled steel fibers with impurities (with a high amount of rubber and textiles) (RSFI) and clean recycled steel fibers (CRSF), have been investigated. Recycled fiber's performance has been compared to industrial steel fibers (ISF); these fibers have hook ends. The mechanical properties of normal concrete and concrete reinforced with steel fibers, including compressive strength, splitting tensile strength, and flexural strength, were investigated at ambient temperature and temperatures of 200 °C and 600 °C. The results showed that at ambient temperature and 200 °C, RSFI decreases the compressive strength of concrete due to the high amount of rubber and textiles, while CRSF has shown results comparable to ISF at all temperatures. The positive effect of RSFI has been observed at 600 °C by melting rubber and burning textiles. The specimens reinforced with steel fibers, regardless of their type, improved the tensile strength and modulus of rupture compared to the control specimen at all temperatures. RSFI has shown poorer performance compared to ISF and CRSF. The mechanical and economic analysis showed that CRSF could be a suitable alternative to ISF to strengthen concrete mixtures.

*Corresponding address: Department of Civil Engineering, Ferdowsi University, Postal code 9177948974, [Azadi Square, Mashhad, Razavi Khorasan Province, Iran](#). Tel.: +985138802415; fax: +985138836056.
E-mail addresses: yaghout.modarres@mail.um.ac.ir; ghalehnovi@um.ac.ir (M. Ghalehnovi)

Keywords: Concrete, Recycled steel fibers, Industrial steel fibers, Waste tires, High temperature.

1. Introduction

Concrete is one of the common elements used in the construction industry. Every construction material has characteristics in which it has advantages or disadvantages (Mohajerani et al., 2019); For instance, the main feature of concrete is its high compressive strength while having low tensile strength (Behfarnia and Behravan, 2014). Concrete always has internal micro-cracks due to temperature and relative humidity changes, which leads to poor tensile strength and consequent brittle failure (Shannag, 2011). One of the most effective ways to strengthen the brittle matrix and prevent cracking is to add natural or synthetic fibers to the concrete mix (Jamshaid and Mishra, 2016; Karimipour et al., 2021). Fibers can be selected based on their properties and added to construction materials to improve the properties of the base material (Mohajerani et al., 2019; Roesler et al., 2006). The use of industrial steel fibers (ISF), which is very common today and requires high raw materials and energy, leads to the adverse environmental effects of CO₂ emissions during production (Frazão, 2019). Therefore, finding fibers with the same function as ISF is essential.

One of the most popular fibers today is recycled fibers from waste materials. Increasing the volume of waste with limited landfills is a known problem due to population growth (Mohajerani et al., 2019). By using waste materials and fiber recycling, the volume of waste can be significantly reduced, and the energy required for the combustion process of landfills can be saved (Mohajerani et al., 2019). Vehicle waste tires are dumped or disposed of worldwide, posing a severe environmental threat. Most waste tires are used as fuel by some industries, but as we know, this type of waste use has a dangerous effect due to the production of greenhouse gases (Frazão, 2019). In recent years, extensive studies have been conducted on using these waste tires in the construction sector (Liew and Akbar, 2020; Awolusi et al., 2021; Modarres and Ghalehnovi, 2022). Products extracted from tires include nylon fibers, nylon pellets, steel fibers, crumb rubber, and rubber powder (Bulei et al., 2018).

The results of studies have shown that recycled steel fibers (RSF) can be slightly helpful for the compressive strength of concrete (Liew and Akbar, 2020; Awolusi et al., 2021). Still, if a large volume of fibers is used, excess water to overcome workability problems can decrease the compressive strength of concrete due to increased porosity (Liew and Akbar, 2020; Awolusi et al.,

2021). Dehghanpour et al. (2018) also showed that for fibers with a fixed length of 25 mm, increasing the fiber content from 0% to 2% increased the compressive strength of concrete. Increasing the content by more than 2% decreased the compressive strength. The amount of rubber bonded to the RSF, the surface morphology, and the fiber form significantly impact concrete's compressive strength (Rossli and Ibrahim, 2012). Some studies have shown that rubber attached to the surface of steel fibers impairs concrete's compressive and tensile strength (Rossli and Ibrahim, 2012; Barros et al., 2017). Rubber particles' hydrophobicity and weak bonding with the surrounding cement matrix negatively impact the concrete performance (Awolusi et al., 2021; Rossli and Ibrahim, 2012). The mixture's fiber content and the type and quality of the fibers used influence fiber-reinforced concrete's post-peak behavior (Awolusi et al., 2021). RSF provides the ability to bridge cracks and stop cracking to improve post-cracking behavior (Wang and Li, 2000). RSF can have comparable results to ISF in energy absorption capacity and residual strength after cracking due to bending load (Aiello et al., 2009). Bedewi (2009) investigated the effect of fiber length and volumetric content on the flexural strength of reinforced concrete with RSF. The results indicated that the maximum fiber length (60 mm) had the highest flexural strength for each desired volume of fibers. Tlemat et al. (2006) studied reinforced concrete's stress-strain properties, compressive strength, and flexural strength with industrial and recycled steel fibers. This study showed that increasing the fiber content reduced the measurement workability. No significant differences were observed for compressive strength, and the flexural behavior of the prisms was improved by increasing the fiber volume.

Engineering structures may be subject to severe loads such as impact, fire, explosion, and combined effects (Ramezani and Esfahani, 2018; Alsaif et al., 2018). The properties of concrete may be significantly affected by high temperatures, which reduces its compressive strength and cracking and spalling (Hager, 2014). In addition, at high temperatures, the bond between the cement paste and the aggregates decreases; The silicate gel, which provides the main strength of the concrete, decomposes, ultimately reducing the concrete's bearing capacity (Bezerra et al., 2019; Handoo and Agarwal, 2002). Insulation boards, coated panels, or sprays are used today to limit spalling in fire or high temperatures (Bezerra et al., 2019). However, fibers are the most effective method to reduce this damage. Fiber improves high-temperature resistance, prevents spalling, limits dimensional variations, and keeps concrete cohesive (Bezerra et al., 2019). Various studies have examined the performance of fiber-reinforced concrete at high temperatures.

The effect of steel fibers on the residual mechanical properties of concrete after exposure to high temperatures and the effect of explosive spalling of concrete during a fire or at high temperatures has been a common topic in recent years. In addition, many types of research have been conducted to investigate the residual properties and behavior of explosive spalling (Wu and Zhou, 2020). When concrete is exposed to fire or high temperatures, steel fibers can reduce the water vapor pressure in the concrete pores and prevent them from growing and spreading by bridging the cracks (Wu and Zhou, 2020; Hossain et al., 2013). Numerous investigations have been conducted on the impact of ISF on the characteristics of concrete subjected to high temperatures (Wu and Zhou, 2020). However, the effect of RSF from waste tires has not been studied much. Yang et al. (2019) investigated ultra-high-performance concrete's mechanical properties and explosive spalling behavior, including different steel fibers. The specimens were heated in a furnace at room temperature up to 800 °C to test for explosive spalling. The results showed that RSF significantly reduced the temperature range and the duration of explosive spalling.

Based on the above, more research is necessary to determine how recycled fibers affect concrete's mechanical performance, particularly at high temperatures. Therefore, this study investigated the compressive strength, splitting tensile strength, and flexural performance of reinforced concrete with RSF from waste tires at ambient and high temperatures. This study also considers reinforced concrete with ISF (hooked-end steel fibers) for better comparison. In addition, an economic analysis has been done to select the appropriate mixture.

2. Experimental program

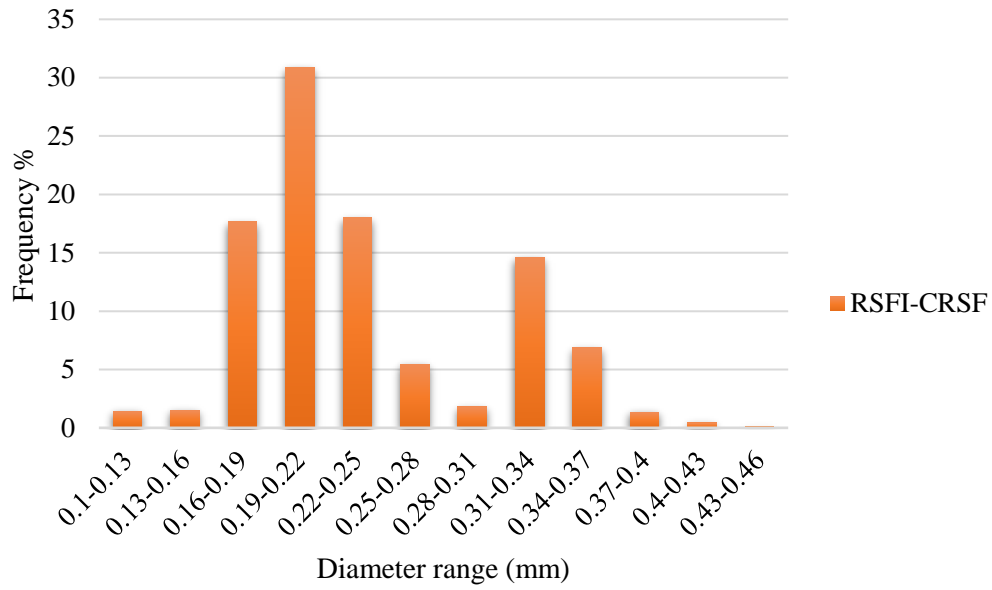
2.1. Materials and mix designs

The recycled fibers used in this study were obtained from the Mashhad waste tire recycling factory. Steel fibers are obtained with the help of the shredding method. In such a way, the bead wire of rubber tires is stretched or cut by the machines, and then the tires without bead wire are directed to the shredder in several different stages. Finally, two types of recycled fibers can be obtained. As shown in Figure 1a, the first type is recycled steel fibers with impurity (RSFI), which are prepared in the early stages of separation; These fibers have a high amount of rubber attached to the surface and textiles. The second type is the fibers obtained in the final stages; They have higher purity and are clean recycled steel fibers (CRSF) with fewer rubber and textile particles (Figure 1b).

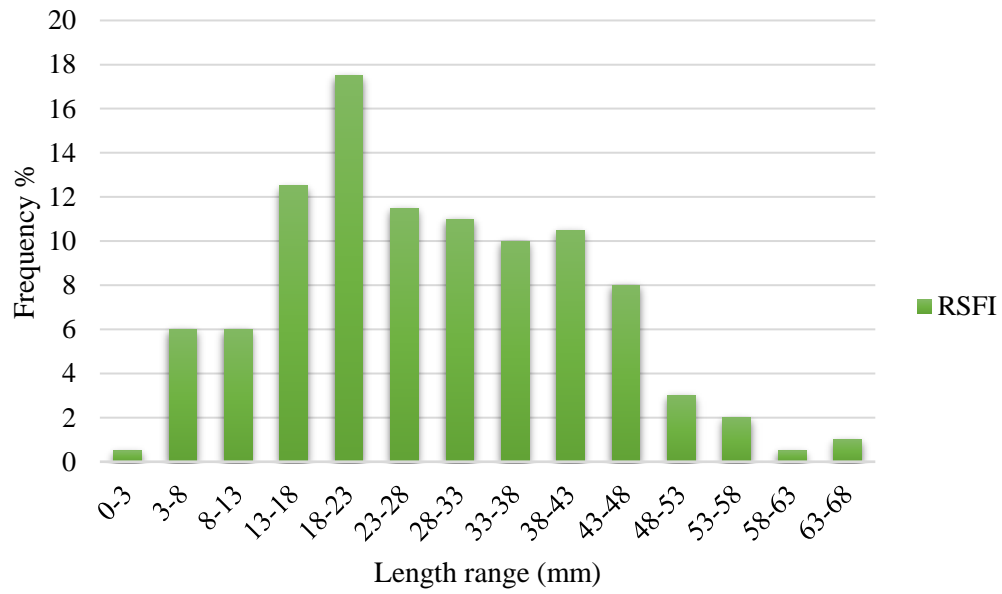


Fig. 1 Steel fibers used: (a) RSFI, (b) CRSF, and (c) ISF

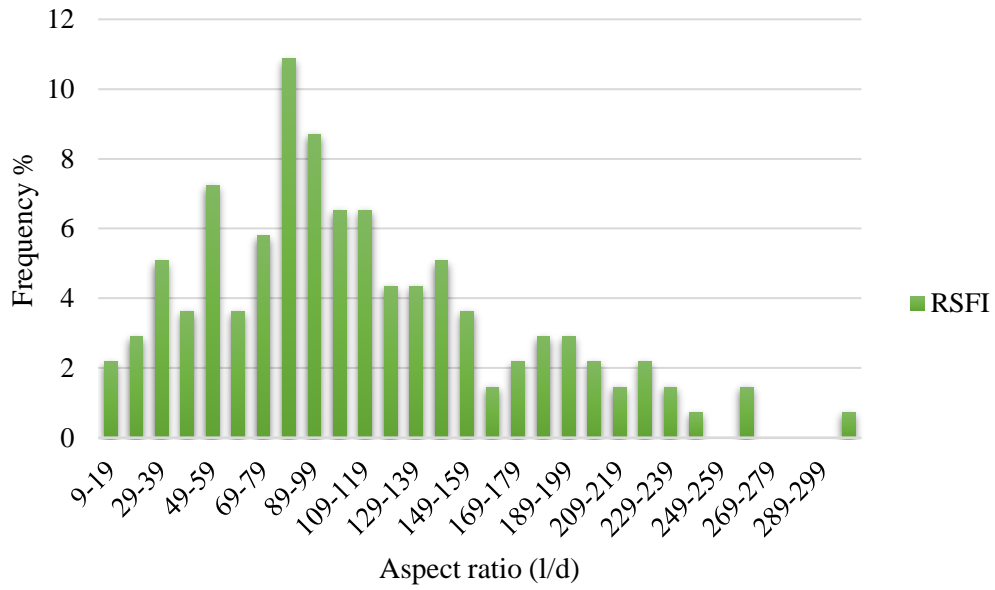
Figure 1 shows that these fibers have irregular shapes and different dimensions. For this reason, 200 fibers were randomly selected as representatives for geometric analysis for both types of fibers. Figure 2 shows the fiber types' length, diameter, and aspect ratio. The fiber's average of both end diameters was measured with a micrometer. Since the fibers have an irregular and distorted shape, the length of the fibers is also considered as the distance between their two outer ends. The measured diameter was the same for both types of fibers. The average fiber diameter was 0.24 mm, with 0.1 mm and 0.46 mm as the lower and upper limits (Figure 2a). 30.87% of the fibers are in the diameter range of 0.19-0.22 mm. RSFI has longer lengths. As shown in Figure 2b, the average fiber length was 28.17 mm, with 3 mm and 67 mm as the lower and upper limits. According to the results, the aspect ratio of these fibers varies in the range of 9.57-300, with an average value of 111.24 (Figure 2c). The average length of CRSF was 21.87 mm, with 2 mm and 47 mm as lower and upper limits (Figure 2d). The aspect ratio of these fibers also varies in the range of 9.66-372, with an average value of 102.66 (Figure 2e). The tensile strength of fibers is also 2488 MPa.



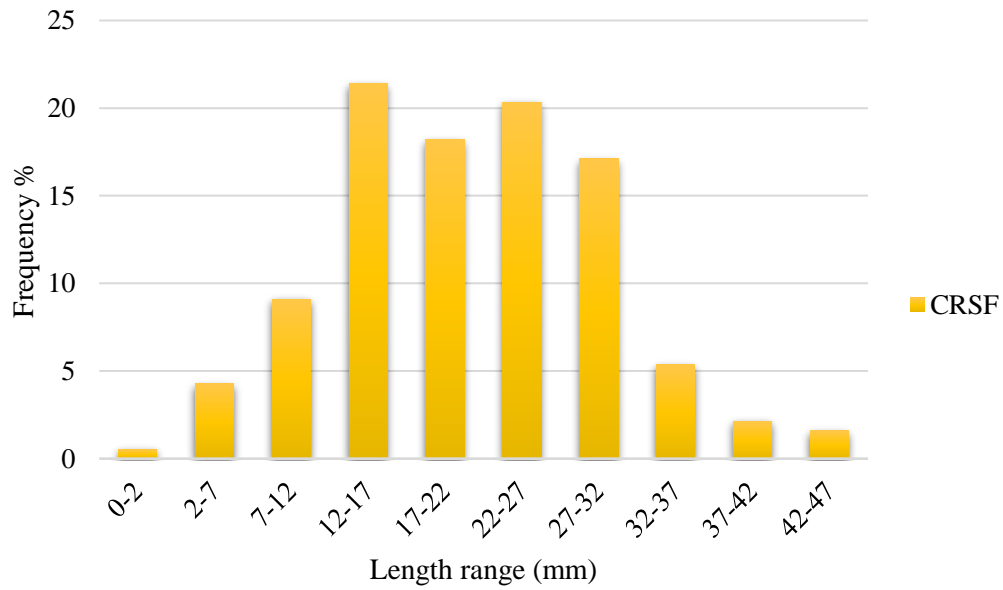
(a)



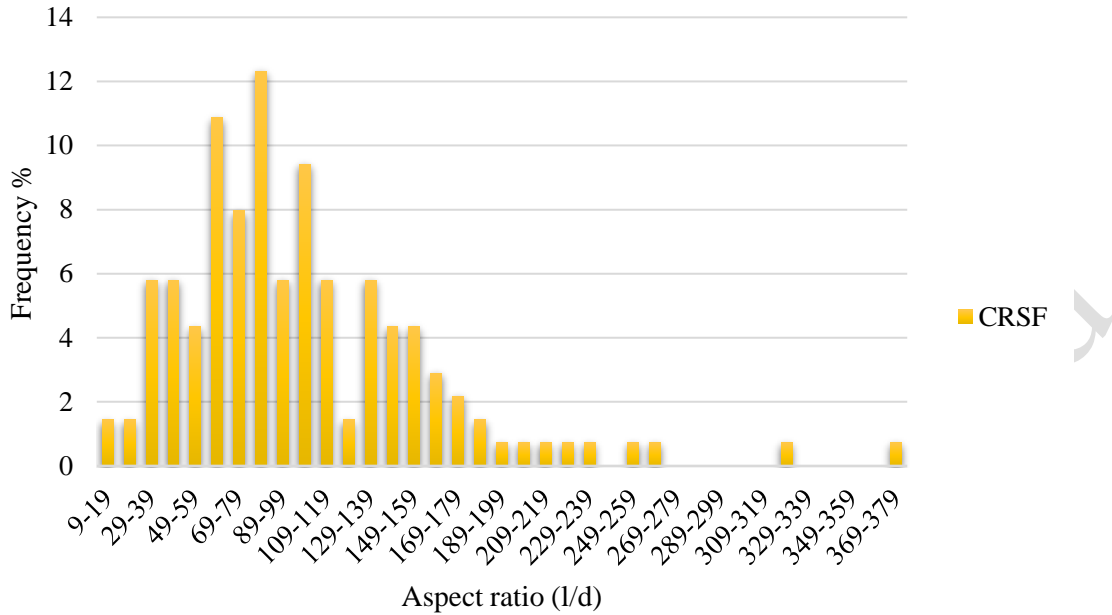
(b)



(c)



(d)



(e)

Fig. 2 Geometric analysis of recycled steel fibers: (a) diameter of RSFI and CRSF, (b) length of RSFI, (c) aspect ratio of RSFI, (d) length of CRSF, and (e) aspect ratio of CRSF

In this study, ISF has also been used to better investigate the effect of recycled fibers. As shown in Figure 1c, these fibers have hooked ends. The supplied company provides the specifications of the industrial fibers. The average diameter of the fibers is 0.8 mm, the length of the fibers is 50 mm, and the aspect ratio is 62.5. The tensile strength of fibers is 1200 MPa.

The mixture ingredients used in this study are Portland cement type II, aggregates, water, and superplasticizer. Recycled and industrial fibers with a volume percentage of 0.5% were used to strengthen the mixtures. In the tests, Zaveh type II cement was used. The coarse aggregates used are broken and obtained from the stone materials suppliers in Mashhad's suburbs. The maximum nominal size of coarse aggregates used was 19 mm. The fine aggregates used were twice washed Sarakhs sand with minimum and maximum sizes of 0.2 and 4.75 mm. In order to maintain the workability of concrete, a superplasticizer based on modified polycarboxylates has been used according to the ASTM C494 standard (2015). The mix design used for this study based on ACI 211 (1991) is given in Table 1. Where NC stands for Normal Concrete, control specimen (without fibers); RSFI stands for Recycled Steel Fibers with Impurities (with rubber attached to the surface and textiles), CRSF stands for Clean Recycled Steel Fibers, and ISF stands for Industrial Steel

Fibers. The numbers written in front of them indicate the volume of the fibers. For example, RSFI-0.5% represents the specimen reinforced with 0.5% recycled steel fibers with impurities.

Table 1 The proportions of mix composition (kg/m³)

Concrete type	W/C	Water	Cement	Sand 0 - 4 mm	Gravel 4 - 19 mm	Steel fiber (%)	Superplasticizer
NC	0.47	180	380	795	1002	0	-
RSFI-0.5%	0.47	180	380	795	1002	0.5	1.9
ISF-0.5%	0.47	180	380	795	1002	0.5	1.52
CRSF-0.5%	0.47	180	380	795	1002	0.5	1.9

2.2. Preparation of specimens and heat treatment

First, the coarse aggregates, fine aggregates, and cement were added to the mixer and mixed for 1 minute. After adding water and superplasticizer, the mixture was mixed for 3 to 5 minutes. The recycled fibers were separated by hand and gradually added to the mix to prevent the fibers from balling inside the mix and ensure their uniform and proper distribution in the concrete matrix. After adding all the fibers, the concrete was mixed for 5 minutes until it was completely homogeneous, and then the mixer was turned off. From each mixture, three cylinders with dimensions of 100 mm × 200 mm were prepared for the compression and tensile test, and three prisms with dimensions of 100 mm × 100 mm × 400 mm were prepared for the flexural test. After 24 hours, specimens were molded, then cured with water at room temperature for 28 days. The specimens were dried in an oven for 24 hours at 60 °C.

Before determining the mechanical behavior of concrete, the specimens were exposed to 200 °C and 600 °C inside an electric heating furnace (Figure 3). To obtain the desired temperature, a heating rate of 1-4 °C/min was applied for all specimens. Then, they were kept at a constant target temperature for 1 hour and a half to ensure uniform temperature distribution in the specimen volume. The specimens were heated, cooled in a furnace to room temperature, and tested the next day.



Fig. 3 Electric heating furnace

2.3. Tests methods

To investigate the compressive strength, according to the ASTM C39 standard (2018), a uniaxial compressive test was performed on cylindrical specimens with dimensions of 100 mm × 200 mm. A hydraulic compression machine with a capacity of 3000 kN with a constant loading rate of 0.3 MPa/s was used for compression tests. Three cylinders were tested for each mixture design to obtain mean values and standard deviation. The splitting tensile test was performed according to the ASTM C496 standard (2004) on cylindrical specimens with dimensions of 100 mm × 200 mm. A constant loading rate of 0.1 MPa/s was applied to all specimens in the test, and the maximum force was recorded. Figure 4a and b exhibit the setup for the compressive and tensile tests. The tensile strength is calculated based on the maximum applied force according to equation 1:

$$f_t = \frac{2P}{\pi Ld} \quad (1)$$

Where P is the maximum tensile force, L is the length of the cylinder (200 mm), and d is the diameter of the cylinder (100 mm).

Figure 4c represents the setup for the flexural tests. Four-point bending tests were performed on prisms with 100 mm×100 mm×400 mm dimensions. The bending load was recorded using a load cell with a capacity of 20 tons. The load was applied uniformly at a 0.2 mm/min rate to obtain the load-deflection curve. The distance between the two upper supports was 100 mm, and the two lower supports were 300 mm. Linear variable differential transducers (LVDT) were installed on both sides of the specimen to measure the mid-span deflection. Three prisms were tested for each mixture design to obtain mean values and standard deviation. Ultimate flexural strength (f_p) or modulus of rupture (MOR) is the flexural stress at peak load, which the following equation can calculate (ASTM C1609, 2012):

$$f_p = \frac{PL}{bd^2} \quad (2)$$

Where P is the peak load, L is the clear span length (300 mm), b is the width of the specimen (100 mm), and d is the depth of the specimen (100 mm).

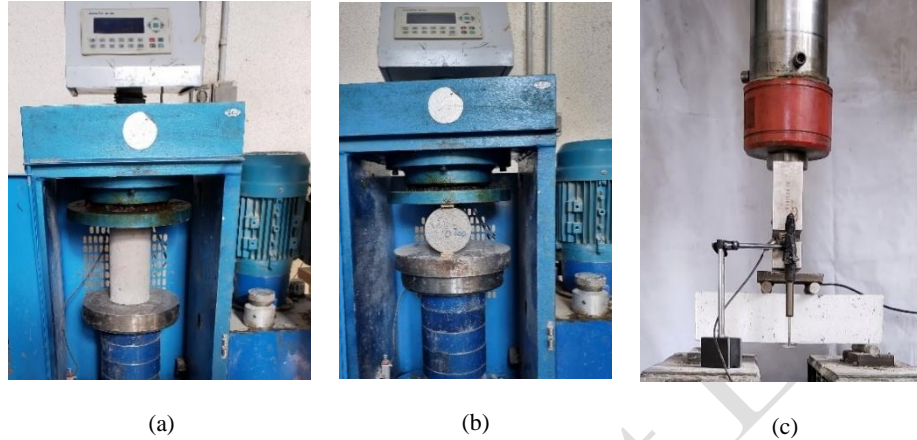


Fig. 4 Setup for: (a) compressive, (b) tensile, and (c) flexural test

According to ASTM C1018 (1997), the toughness indices I_5 , I_{10} , and I_{20} can be obtained based on the load-deflection curve as follows:

$$I_5 = \frac{A_{3\delta}}{A_\delta} \quad (3)$$

$$I_{10} = \frac{A_{5.5\delta}}{A_\delta} \quad (4)$$

$$I_{20} = \frac{A_{10.5\delta}}{A_\delta} \quad (5)$$

Where δ is the deflection of the first crack; A_δ , $A_{3\delta}$, $A_{5.5\delta}$, and $A_{10.5\delta}$ are the area under the load-deflection curve up to δ , 3δ , 5.5δ , and 10.5δ , respectively. Residual strength factors can be obtained from toughness indices (ASTM, 1997). These factors represent the resistance retained after the first crack with the help of the average post-crack load in a specific deflection interval. Residual strength factors $R_{5,10}$ and $R_{10,20}$ can be calculated from the value of $20(I_{10} - I_5)$ and $10(I_{20} - I_{10})$, respectively.

3. Discussion and results

3.1. Appearance of specimens and cracking at high temperatures

In order to investigate the influence of fibers on cracking and spalling behavior, the specimens were heated in an electric heating furnace at a rate of 4 °C/min to a temperature of 800 °C. Then the specimens' color, cracking, and spalling were checked at different temperatures. As shown in Figure 5, the specimens were gray at the temperature of 200 °C, and no significant color change occurred. Cracking and spalling did not occur in the control and fiber-reinforced specimens. At the temperature of 400 °C, the color of the specimens was gray-brown. Micro-cracks were visible on the surface of the specimens. The specimens reinforced with ISF had less cracking than those reinforced with recycled fibers. At 600 °C, the color of the specimens was light gray. At this temperature, micro-cracks joined together and formed macro-cracks. Spalling and loss of corners had occurred in some control and reinforced with recycled fibers specimens.

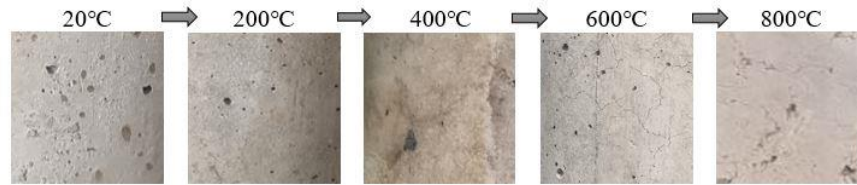


Fig. 5 Color change of specimens at different temperatures

At 800 °C, no explosive spalling occurred for the specimens. The morphology of all specimens after exposure to 800 °C is shown in Figure 6. The results show that using RSF can reduce the intensity of cracking and spalling of the surface of the specimens. Textiles and rubbers attached to the surface of the fibers melt completely at 800 °C. They can create open pores inside the concrete, which leads to easier evaporation of water vapor and helps reduce internal pore pressure. Deep cavities, macro-cracks, and spalling are visible on the surface of the specimens. The depth of the control specimens' cavities is more significant than those reinforced with recycled fibers. The specimens reinforced with CRSF and ISF showed similar and close performance.

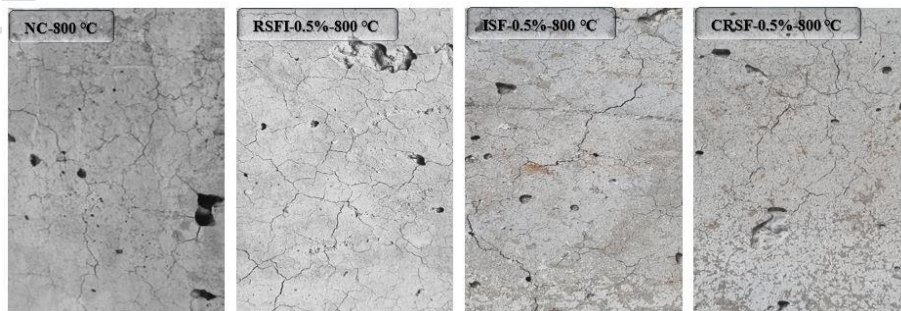


Fig. 6 Morphology of specimens after subjected to a temperature of 800 °C

3.2. Mass loss of specimens

In this study, the mass loss rate of cylindrical specimens has been evaluated as the ratio of the mass loss at high temperatures to the initial mass of the specimen at ambient temperature. Six specimens were weighed before and after exposure to high temperatures for each mixture. Figure 7 shows the mass loss of the specimens at different temperatures. At a temperature of 200 °C, the mass loss of the specimens is low. The decrease in mass at this temperature is related to the evaporation of free water in the pores and aggregates (Mastali et al., 2018a; Memon et al., 2019). The average mass loss percentage of the control specimen at a temperature of 200 °C is about 1.72%, but the mass loss is more for specimens reinforced with fibers. Fibers inside the concrete create pores and empty spaces due to difficult compaction (Mastali et al., 2018a).

On the other hand, the compaction of concrete with recycled fibers is more difficult due to the presence of rubber and textiles. The average mass loss percentage for specimens containing recycled fibers was 3.59%, and for industrial fibers was 3.49%. Recycled fibers have textiles and rubber attached to the surface; Some textiles, which are close to the surface, burn at this temperature and can cause mass loss.

At the temperature of 600 °C, the highest mass loss is related to RSFI-0.5%, with a value of 8.80%. At this temperature, all rubbers and textiles burn entirely, which leads to porosity and, as a result, a significant mass loss. At 600 °C, the chemical bond of water is destroyed, and calcium hydroxide is dehydrated and decomposed (Memon et al., 2019). The dehydration of silicate gel is also progressive, completely dehydrated, and decomposed at approximately 600-700 °C (Memon et al., 2019). In addition, concrete loses all its capillary water at temperatures above 400 °C (Memon et al., 2019). The mass loss rate of NC and CRSF-0.5% specimens are close and 7.47% and 7.34%, respectively.

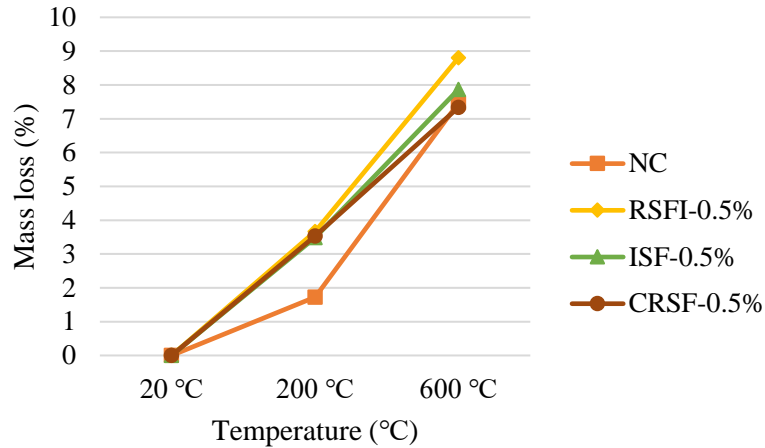
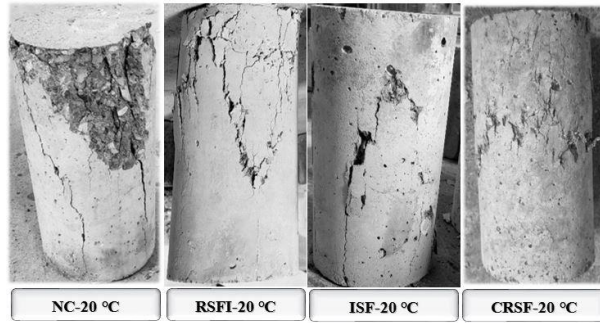


Fig. 7 Mass loss of specimens at different temperatures

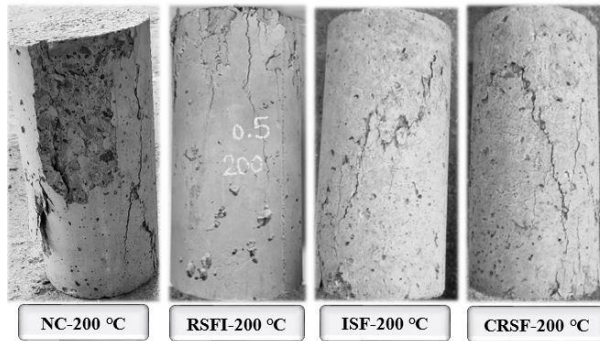
3.3. Compressive strength at ambient and high temperatures

The results of the compressive failure mode for the control and fiber-reinforced specimens at different temperatures are shown in Figure 8. The results show that the specimens reinforced with ISF and CRSF have higher compressive strength than NC and RSFI at all temperatures. The failure mode of the control specimen was brittle and unexpected at all temperatures, and parts of the specimens were separated and scattered around. While specimens are reinforced with fibers, regardless of the type of steel fibers, the brittle failure mode becomes ductile because steel fibers prevent the propagation and joining of cracks and maintain the integrity of the specimens.

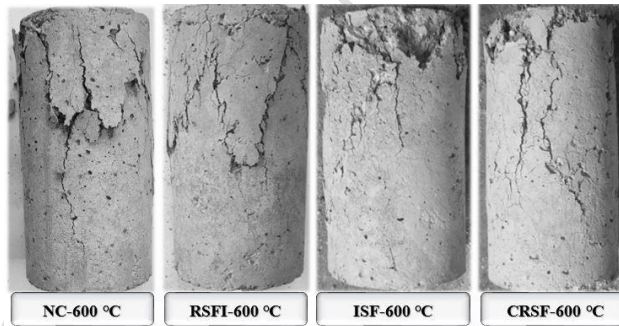
In general, the results show that at ambient and high temperatures, CRSF has shown a performance close to ISF in improving the compressive strength of concrete. As shown in Figure 9, at ambient temperature, ISF-0.5% and CRSF-0.5% compressive strength is 27.73% and 29.53% higher than NC, respectively. Meanwhile, at ambient temperature and 200 °C, the compressive strength of RSFI-0.5% is 6.18% and 19.17% lower than NC, respectively. This decrease in compressive strength can be related to the high amount of rubber attached to the surface of fibers and textiles. Rubber forms a weak bond with the surrounding cement matrix, which leads to an increase in porosity and, as a result, a decrease in strength (Zhang et al., 2020; Fu et al., 2019).



(a)



(b)



(c)

Fig. 8 Compressive failure mode of specimens: (a) Ambient temperature, (b) 200 °C, (c) 600 °C

At ambient temperature, the compressive strength of specimens reinforced with CRSF and ISF is close. However, at a temperature of 200 °C, the compressive strength of CRSF-0.5% is 7.44% lower than ISF-0.5%. Compared to RSFI, CRSF is cleaner fibers but still contains less rubber and textiles. Textiles close to the surface of the specimen burn at 200 °C and can lead to micro-cracks and porosity and, as a result, decrease in strength compared to ISF-0.5% specimens.

At a temperature of 600 °C, a sharp drop in strength can be seen for all specimens. The lowest value of residual compressive strength is related to NC, with a value of 12.87 MPa; the highest

value is CRSF-0.5%, with a value of 19.67 MPa. The residual compressive strength of RSFI-0.5% is 6.53% higher than NC at this temperature. The positive role of the presence of rubber and textiles with fibers can be seen at high temperatures. Rubber and textiles melt at a temperature of 600 °C and create a network of open pores inside the concrete, which helps escape the formed water vapor more efficiently and can reduce cracking and spalling caused by pore pressure (Wu and Zhou, 2020; Hossain et al., 2013). Of course, it is essential to mention that the complete melting of the rubber attached to the surface of the fibers reduces the bond between the cement paste and the fibers. Therefore, this issue can also justify the reduction of the compressive strength of specimens reinforced with RSFI compared to CRSF and ISF. The results of the average compressive strength of the specimens at different temperatures are presented in Table 2.

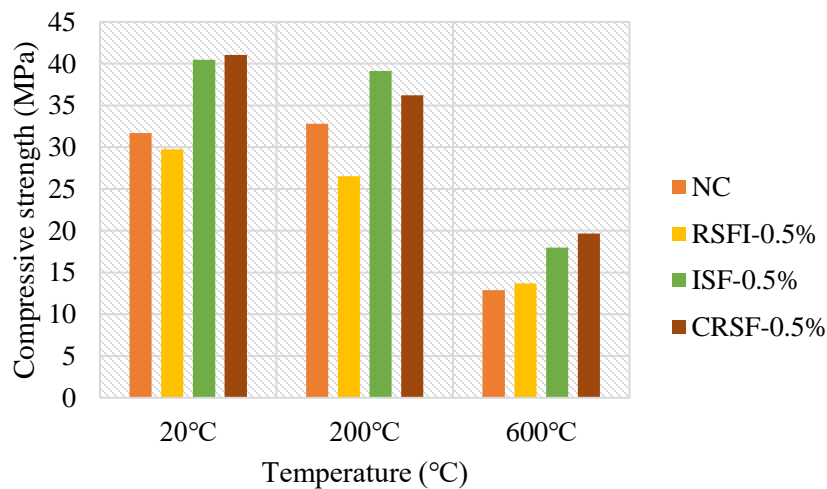


Fig. 9 Compressive strengths of specimens at different temperatures

Table 2 Average mechanical properties of concrete at different temperatures (MPa)

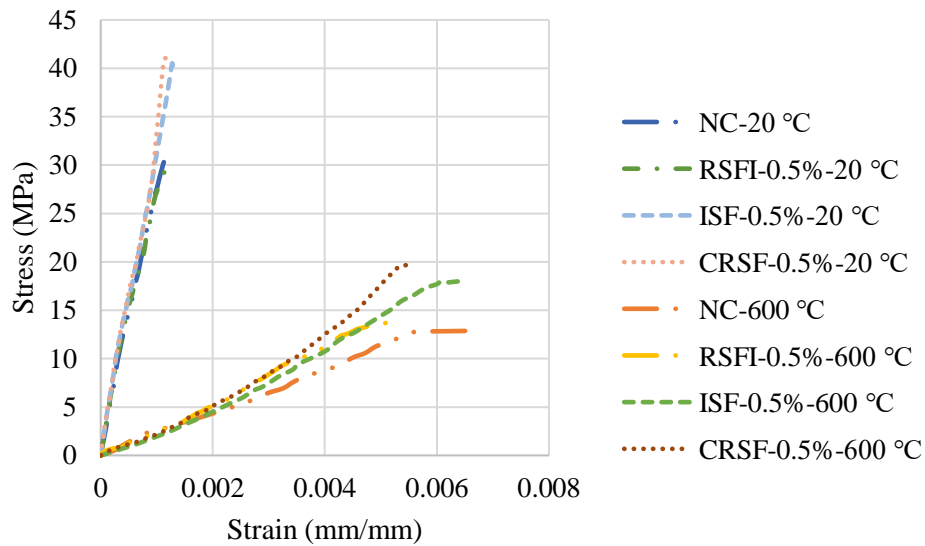
Concrete mixes	Compressive strength (MPa)					Splitting tensile strength (MPa)				
	Temperatures			Reduction rate (%)*		Temperatures			Reduction rate (%)*	
	20 °C	200 °C	600 °C	200 °C	600 °C	20 °C	200 °C	600 °C	200 °C	600 °C
NC	31.70	32.81	12.87	3.50	-59.40	4.59	3.59	1.04	-21.79	-77.34
RSFI-0.5%	29.74	26.52	13.71	-10.83	-53.90	4.67	3.61	1.46	-22.70	-68.74
ISF-0.5%	40.49	39.12	17.98	-3.38	-55.59	4.77	4.18	1.72	-12.37	-63.94
CRSF-0.5%	41.06	36.21	19.67	-11.81	-52.09	4.68	3.62	1.64	-22.65	-64.95

*The rate of resistance reduction compared to the ambient temperature

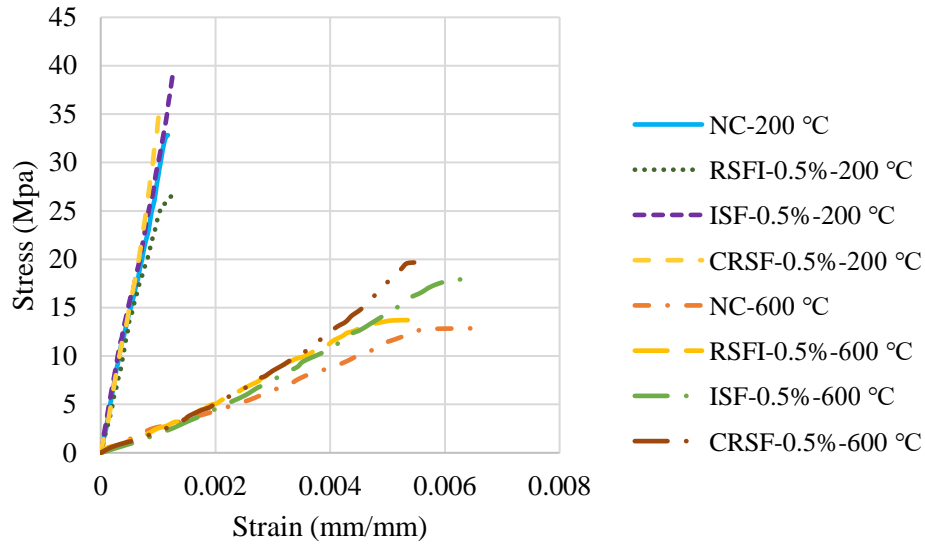
3.3.1. Stress-strain curve and secant modulus of elasticity

The stress-strain diagrams related to the force-displacement values obtained during the compressive test are drawn in Figure 10. The modulus of elasticity of concrete is determined with

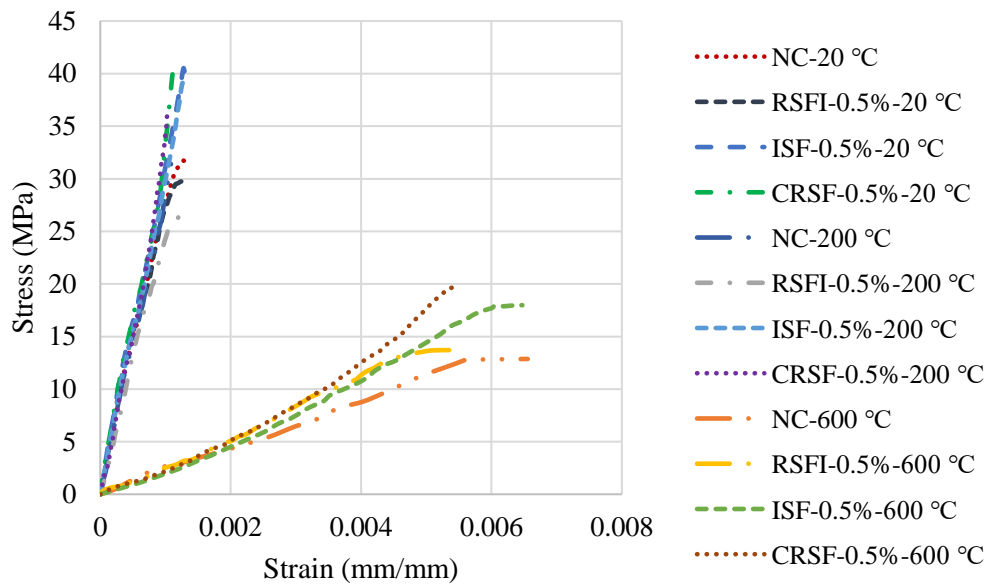
the help of compressive tests of cylindrical specimens. The secant modulus is the slope of the line that connects from the origin to the point of the curve, such as 40% of the ultimate rupture stress. The results have shown that the compressive strength and modulus of elasticity decrease with increasing temperature while the strain related to the maximum compressive stress increases. For all specimens at 200 °C, the strain corresponding to the maximum compressive stress is close to the ambient temperature strain, and only a tiny amount has increased. For example, the strain increase for RSFI-0.5% at 200°C is 0.45% compared to ambient temperature. Nevertheless, at a temperature of 600 °C, the increase in strain related to the maximum compressive stress is significant. At this temperature, the average strain increase (for all specimens) compared to the ambient temperature is 390.17%.



(a)



(b)



(c)

Fig. 10 Comparison of stress-strain curves of specimens at different temperatures: (a) 20 °C vs 600 °C , (b) 200 °C vs 600 °C, (c) all temperatures

At high temperatures, the modulus of elasticity decreases due to the formation of micro-cracks and the thermal degradation of concrete components (Zhang et al., 2020). At temperatures below 400 °C, the vapor pressure caused by the evaporation of free water in the concrete is the main factor in reducing the compressive strength and modulus of elasticity (Ma et al., 2015). At a temperature

higher than 400 °C, cracks in the interfacial transition zone (ITZ) caused by thermal reactions between the aggregate and the cement matrix and the fibers and the cement matrix lead to a decrease in compressive strength and elastic modulus. Figure 11 shows the modulus of elasticity for specimens at different temperatures.

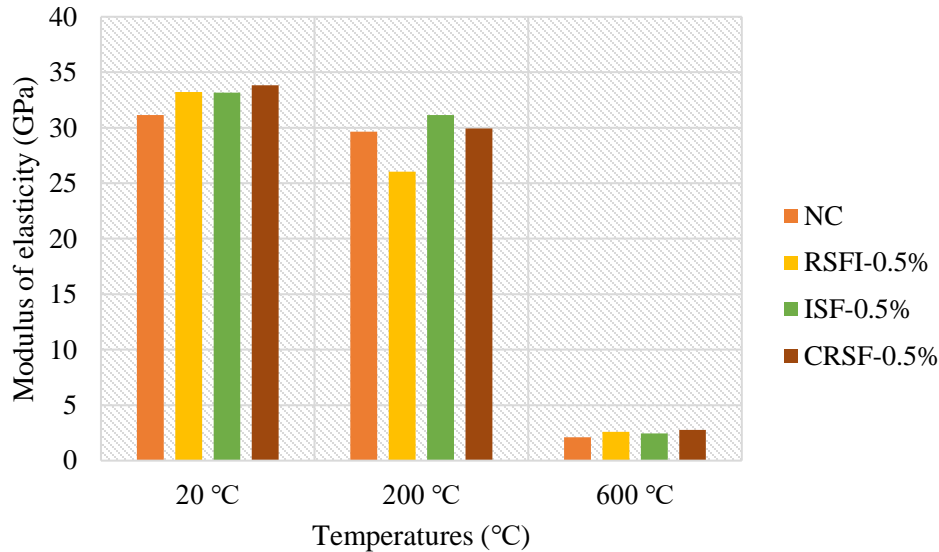


Fig. 11 The secant modulus of elasticity of the specimens at different temperatures

The reduction of the modulus of elasticity at 200 °C is small. The lowest decrease in modulus of elasticity is related to NC, and the highest amount is related to RSFI-0.5%. At a temperature of 600 °C, a sharp decrease in the modulus of elasticity is observed. Using fibers at high temperatures has improved the modulus of elasticity compared to the control specimen. The elastic modulus of RSFI-0.5%, ISF-0.5%, and CRSF-0.5% is 21.29%, 15.21%, and 26.72% higher than NC at this temperature, respectively. At a temperature of 600 °C, the value of the drop of the modulus of elasticity for specimens reinforced with fibers can be considered the same.

3.4. Splitting tensile strength at ambient and high temperatures

Figure 12 shows how tensile cracks are formed in specimens at different temperatures. All cracks occurred in the middle of the section, close to the diameter. In NC and RSFI-0.5% at 600 °C, the cracks were deeper, and near the cross-section wall, the cracks have spread in the form of branches. Steel fibers (regardless of their type) have partially prevented the branching growth of cracks at high temperatures.

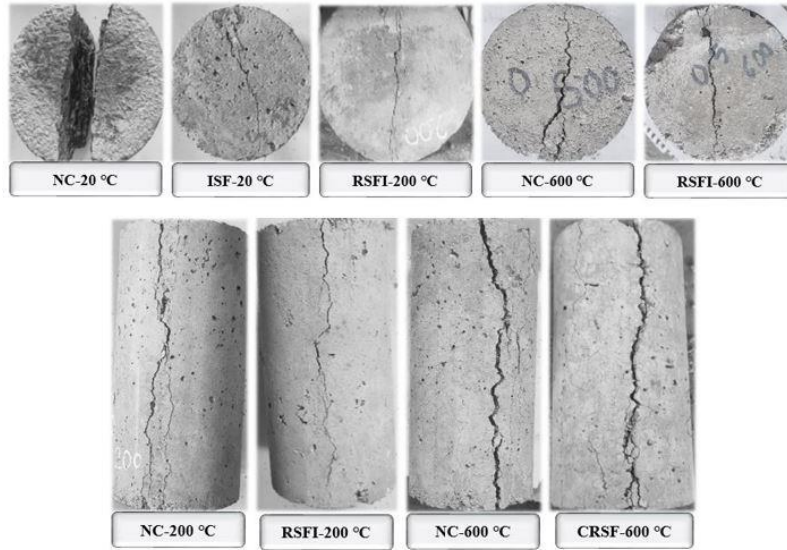


Fig. 12 Tensile failure mode of specimens at different temperatures

The results have shown that adding steel fibers (regardless of their type) has improved tensile strength at all temperatures. Figure 13 shows the tensile strength results of the control and fiber-reinforced specimens at different temperatures. At ambient temperature, the tensile strength of all specimens is close to each other. The highest tensile strength is related to ISF-0.5%, with a value of 4.77 MPa, and the lowest is related to NC, with a value of 4.59 MPa. As the temperature increases, the tensile strength of the specimens decreases, but the amount of this decrease is lower for the fiber-reinforced specimens than for the control specimens. At ambient temperature and 200 °C, the performance of CRSF-0.5% is only slightly higher than RSFI-0.5%, and generally, they have shown similar performance. However, both fibers have improved tensile strength compared to NC.

At a temperature of 200 °C, the residual tensile strength of ISF-0.5% has decreased to 12.37%. This is while the average strength reduction of specimens reinforced with recycled fibers reaches 22.67%. The recycled fibers' short length and small diameter and the presence of rubber and textiles can be the reason for the more significant decrease in residual tensile strength at this temperature compared to industrial fibers.

At a temperature of 600 °C, a significant drop in residual tensile strength is observed for all specimens. CRSF-0.5% has provided close and comparable performance at this temperature with ISF-0.5%. The residual tensile strength of RSFI-0.5%, ISF-0.5%, and CRSF-0.5% is 40.38%, 65.38%, and 57.69% more than the NC at this temperature. Overall, the results illustrate that the

presence of rubber and textiles did not harm the tensile performance compared to the control specimen. However, the performance of these fibers was slightly weaker compared to industrial fibers. Table 2 displays the findings of the average tensile strength of the specimens at various temperatures.

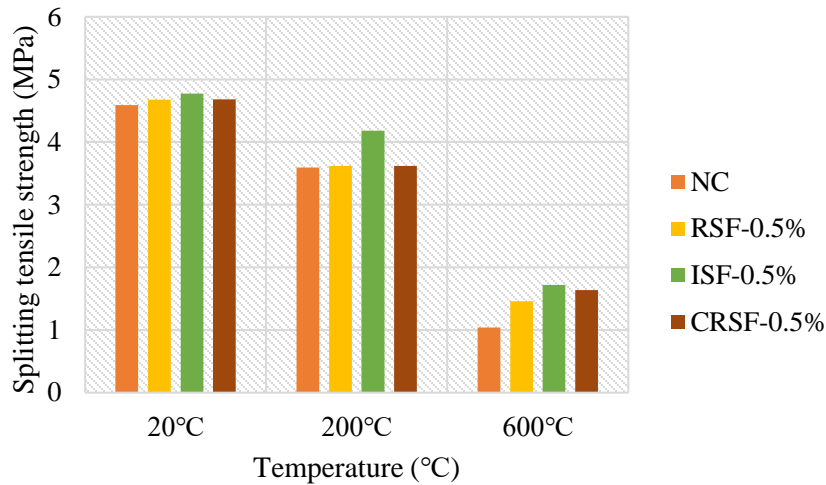


Fig. 13 Splitting tensile strength of specimens at different temperatures

3.5. Flexural strength at ambient and high temperatures

As shown in Figure 14a, the control specimen showed brittle behavior at all temperatures and failed suddenly after reaching the maximum load. Specimens reinforced with fibers have shown semi-brittle behavior at all temperatures; Figures 14b and c show how cracks grow at 200 °C for specimens reinforced with recycled fibers. By bridging the cracks, steel fibers prevent their unstable growth and thus improve the ductility and flexural strength of the prism beams. Figure 14d shows how the fibers bridge the cracks.

The load-deflection curve obtained from the four-point bending test for prismatic specimens at different temperatures is shown in Figure 15. The results show that adding steel fibers increases the peak load compared to the control specimen. All temperatures' highest peak load value corresponds to CRSF-0.5%, followed by ISF-0.5%. Since NC specimens undergo sudden failure, they have a slight ultimate deflection compared to fiber-reinforced specimens. The ultimate deflection of NC specimens at ambient temperature, 200 °C, and 600 °C is 0.32, 0.55, and 2.34 mm, respectively. In comparison, the ultimate deflection of fiber-reinforced specimens is more than 6 mm at ambient temperature and 200 °C and more than 3 mm at 600 °C.

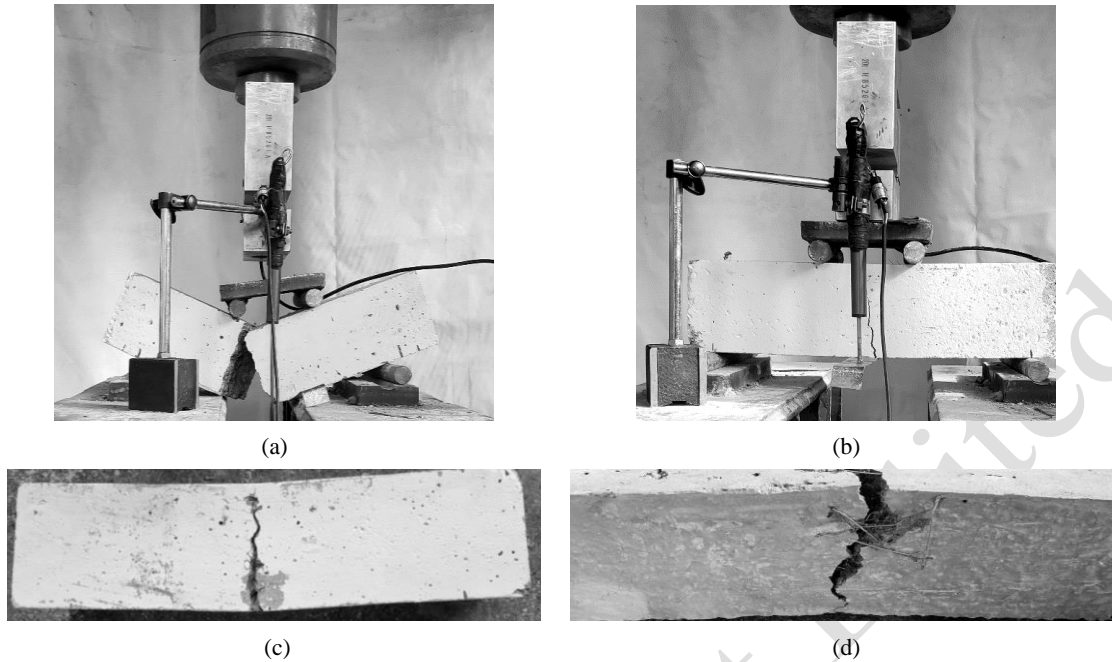
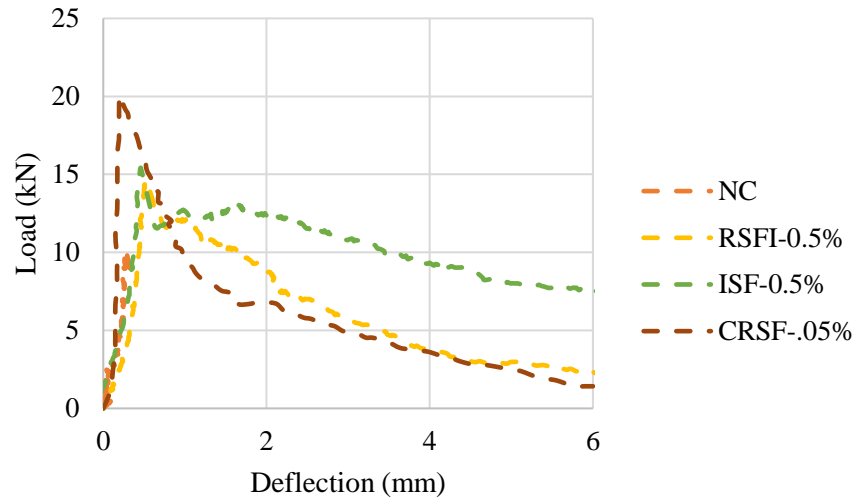


Fig. 14 Cracking of prism beams at 200 °C: (a) NC, (b) RSFI-0.5%, (c) CRSF-0.5%, and (d) ISF-0.5%

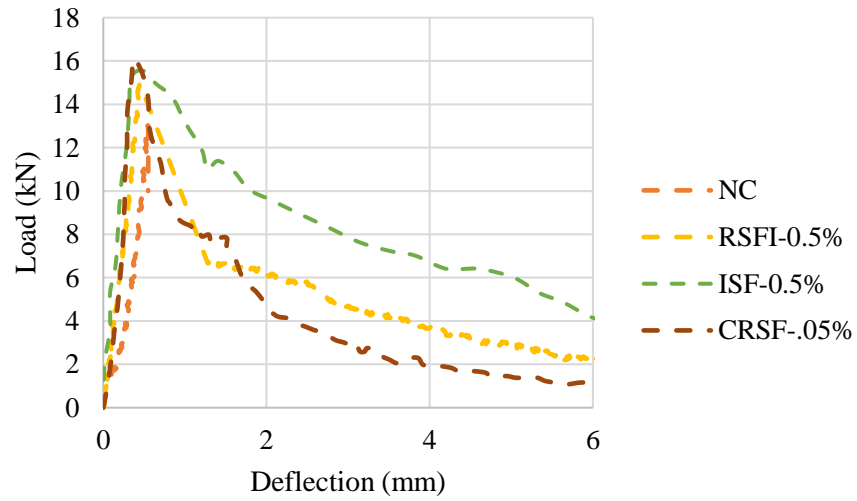
According to the load-deflection diagrams, the slope of the tangent to the curve is defined as flexural stiffness. In general, the results show that the flexural stiffness of all specimens decreases with increasing temperature. This behavior can be related to the decomposition of calcium hydroxide in cement paste and the release of chemical bonding water at higher temperatures (Memon et al., 2019). The most significant decrease in flexural stiffness is related to NC. In contrast, the reduction in flexural stiffness of specimens reinforced with fibers is less. According to Figure 15a, the highest flexural stiffness at ambient temperature corresponds to CRSF-0.5%. At a temperature of 200 °C, the flexural stiffness of the specimens reinforced with fibers is close to the same (Figure 15b). At the temperature of 600 °C, the flexural stiffness of RSFI-0.5% and ISF-0.5% specimens is close to the same (Figure 15c).

Using equation 7, MOR was calculated for specimens at different temperatures. The results show that steel fibers (regardless of their type) have significantly increased the MOR compared to the control specimen at all temperatures. As shown in Figure 16, at ambient temperature, the highest MOR corresponds to CRSF-0.5% with a value of 5.99 MPa, and the lowest MOR corresponds to NC with a value of 3.05 MPa. RSFI-0.5% also significantly improved MOR with the presence of rubber and textiles and increased MOR at ambient temperature by 44.59% compared to NC.

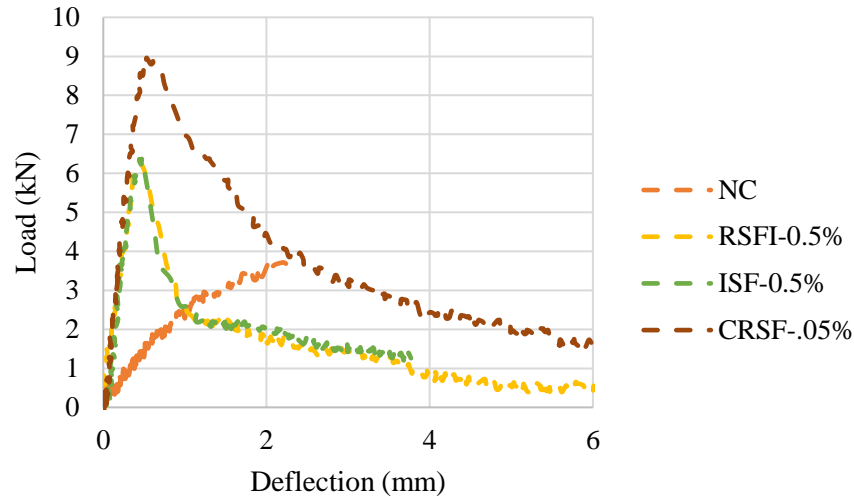
However, it still performs less than ISF-0.5% and CRSF-0.5%. ISF-0.5% at ambient temperature has increased MOR by 51.47% compared to NC.



(a)



(b)



(c)

Fig. 15 Load-deflection curve of specimens at different temperatures: (a) 20 °C, (b) 200 °C, and (c) 600 °C

At the temperature of 200 °C, MOR has increased slightly for all specimens except CRSF-0.5%. The results of other studies have also shown that at a temperature of 200 °C, the strength of specimens reinforced with steel fibers has increased compared to the ambient temperature (Fu et al., 2019). Fiber-reinforced specimens have shown similar performance at this temperature and have increased MOR by 19.40% on average compared to NC. At 600 °C, a severe drop in MOR has been observed for all specimens. The reduction of MOR for NC, RSFI-0.5%, ISF-0.5%, and CRSF-0.5% compared to ambient temperature is 63.61%, 56.92%, 44.80%, and 40.23%, respectively. Table 3 shows the specimens' average peak load and MOR at different temperatures.

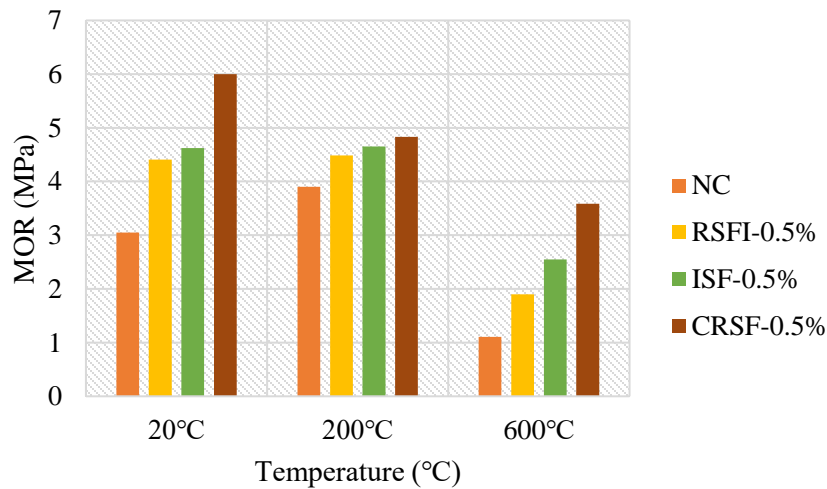


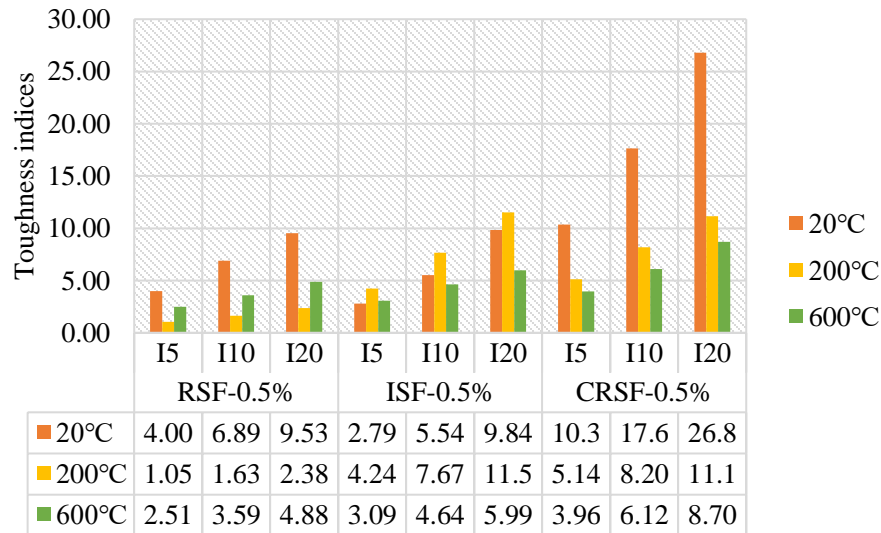
Fig. 16 MOR of specimens at different temperatures

Table 3 Average MOR of specimens at different temperatures (MPa)

Concrete mixes	Peak load (kN)			MOR (MPa)		
	20 °C	200 °C	600 °C	20°C	200 °C	600°C
NC	10.16	13.01	3.69	3.05	3.90	1.11
RSFI-0.5%	14.69	14.96	6.32	4.41	4.49	1.90
ISF-0.5%	15.41	15.51	6.37	4.62	4.65	2.55
CRSF-0.5%	19.99	16.11	8.96	5.99	4.83	3.58

3.5.1. Toughness indices and residual resistance factors

The ductility of the specimens was evaluated based on ASTM C1018 (1997). The toughness indices I_5 , I_{10} , and I_{20} for fiber-reinforced specimens are shown in Figure 17. The control specimens fail suddenly, and their deflection is slight; Hence, their toughness indices values are ignored. The results show that increasing the temperature reduces the toughness indices; But the toughness indices value for RSFI -0.5% at 600 °C is more than 200 °C; At a temperature above 200 °C, the melting of rubber on the surface of the fibers leads to the strengthening of their bond with the cement matrix, which can also help to improve its flexural performance (Fu et al., 2019; Zhang et al., 2020). ISF-0.5% toughness indices are higher than RSFI-0.5% at all temperatures, while the toughness indices of CRSF-0.5% is higher than ISF-0.5% at all temperatures. The average decrease in toughness indices for RSFI-0.5% at 200 °C compared to ambient temperature is 75.07%, and for CRSF-0.5% is 54.13%.

**Fig. 17** Toughness indices at different temperatures

The residual resistance factors $R_{5,10}$ and $R_{10,20}$ show the average resistance level maintained after the first crack as a percentage of the resistance of the first crack. 100 values represent entirely plastic behavior (ASTM, 1997). Low performance is indicated by lower values (ASTM, 1997). The control specimen has a zero residual resistance factor (ASTM, 1997). Table 4 shows the values of the residual resistance factors $R_{5,10}$ and $R_{10,20}$. At ambient temperature, CRSF-0.5% showed plastic behavior.

Table 4 Residual resistance factors at different temperatures

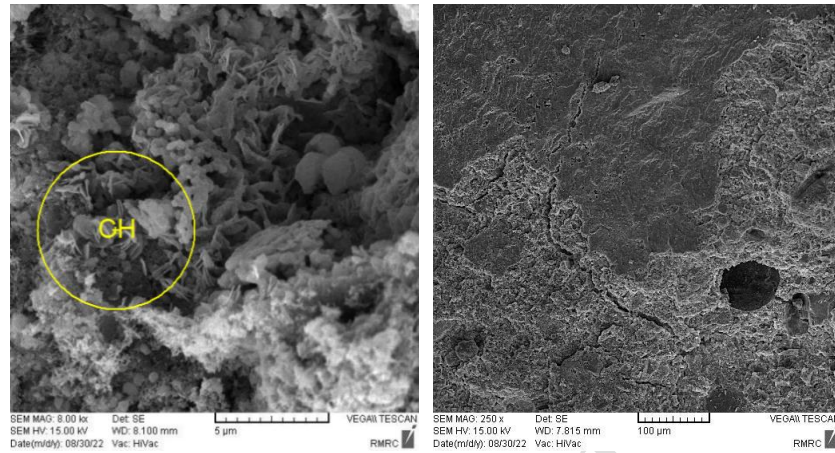
Concrete mixes	Maximum heating temperatures (°C)					
	20 °C		200 °C		600 °C	
	$R_{5,10}$	$R_{10,20}$	$R_{5,10}$	$R_{10,20}$	$R_{5,10}$	$R_{10,20}$
RSF-0.5%	57.77	26.36	11.54	7.53	21.58	12.89
ISF-0.5%	54.98	43.02	68.68	38.56	31.07	13.43
CRSF-0.5%	145.69	91.53	61.18	29.43	43.04	25.86

3.6. Microstructure of concrete at ambient and high temperatures

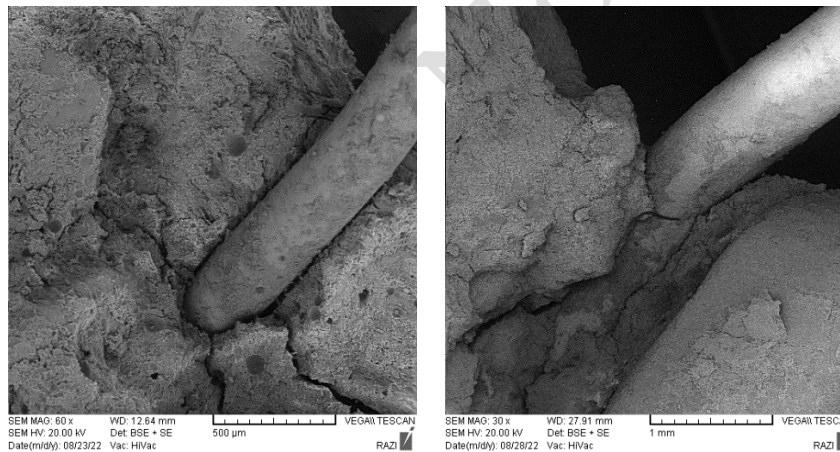
With the help of scanning electron microscopy (SEM), the microstructure of the control and fiber-reinforced specimens at a temperature of 600 °C have been examined. Calcium hydroxide decomposes into CaO and water at 350-550 °C (Xing et al., 2015). Silicate gel, which forms the main strength of concrete, decomposes in the temperature range of 400-600 °C. Figure 18a shows the presence of calcium hydroxide at a temperature of 600 °C in the microstructure of the control specimen. The reason for observing calcium hydroxide can be related to the rehydration of CaO with ambient humidity inside the specimen, which occurred after the specimens were taken out of the furnace and exposed to ambient temperature. This issue is also mentioned in the results found in the Xing et al. study (2015).

In the control specimen, cracking can be seen in ITZ between aggregate and cement paste and inside the aggregate. In specimens reinforced with fibers, ITZ between aggregate and cement paste and between fibers and cement paste is essential. At a temperature of 600 °C, significant changes are observed in the bonding of fibers and cement matrix. As can be seen in Figure 18b, cracking in ITZ between RSFI and cement matrix is more than in the specimens reinforced with ISF and CRSF. The rubber attached to the RSFI surface melts at temperatures above 200 °C. In this case, the bond between fibers and cement matrix is improved. Nevertheless, these rubbers burn completely at 400 °C and above, creating porosity and pores between the fibers and the cement

matrix. As a result, it causes weaker bonding and more cracks in ITZ than ISF (Figure 18c) and CRSF (Figure 18d). In general, the microstructure analysis shows that the cracking of the control specimen is much higher than that of the specimens reinforced with fibers. Steel fibers maintain their properties at high temperatures and prevent cracks' growth and expansion by bridging them.

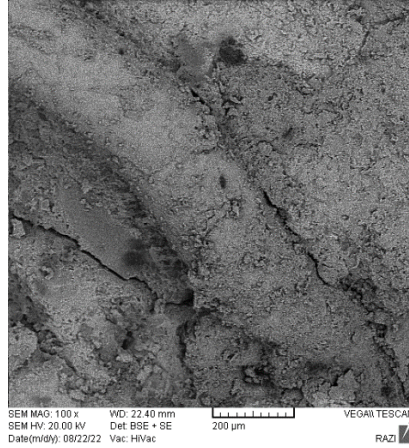


(a)



(b)

(c)



(d)

Fig. 18 SEM observations for specimens at 600 °C: (a) NC, (b) RSFI, (C) ISF, (d) CRSF

3.7. Economic analysis

When introducing and using new materials to strengthen and make concrete, in addition to examining their effect on the mechanical properties of concrete, it is also essential to investigate the impact on the cost of mixtures and global warming potential. In order to find an economical and affordable mixture, the cost of the mixture was calculated considering the cost of the materials used. Since the same mixture design is considered for all mixtures, the most influential parameter in the economic analysis is the unit price of fibers and superplasticizer. The cost of mixtures can be calculated by multiplying the fiber content by the unit price of fibers. The supplier company and the tire recycling factory provide information about the price of industrial and recycled steel fibers. To calculate the cost of mixtures, the cost of each mixture is normalized based on the maximum cost of materials (i.e., superplasticizer). Table 5 shows the normalized unit price. The highest mixture cost is related to ISF-0.5%, and the lowest belongs to RSFI-0.5%. Adding ISF increases the manufacturing cost significantly. Replacing industrial fibers with recycled fibers reduces the cost of mixtures.

Table 5 Normalized cost of mixtures

Mixtures	RSFI-0.5%	ISF-0.5%	CRSF-0.5%
Normalized cost	7.58	40.65	9.55

Furthermore, mechanical properties and the cost of selecting the appropriate mixture should be considered. For this purpose, the compressive strength gain and MOR gain (compared to the

control specimen) per cost unit were calculated and compared for all mixtures at different temperatures. As mentioned in Section 3.3, RSFI leads to a decrease in compressive strength; Therefore, as shown in Figure 19a, the compressive strength gain is negative. Therefore, the ratio of compressive strength gain per unit cost is negative. MOR gain is less for RSFI compared to ISF and CRSF. However, due to its lower cost than ISF, it has a higher ratio of MOR gain to unit cost than ISF (Figure 19b). The results show that using RSFI for flexural members in structures at ambient temperature and after exposure to high temperatures can benefit resistance and economy.

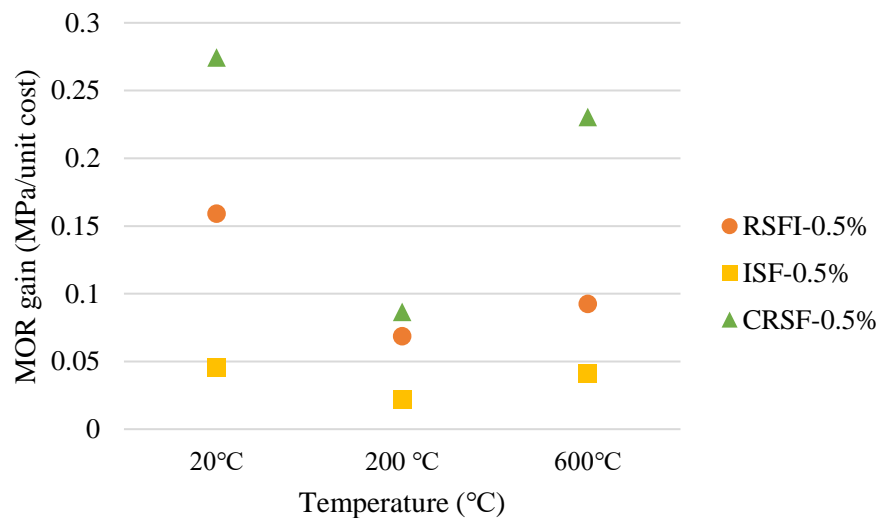
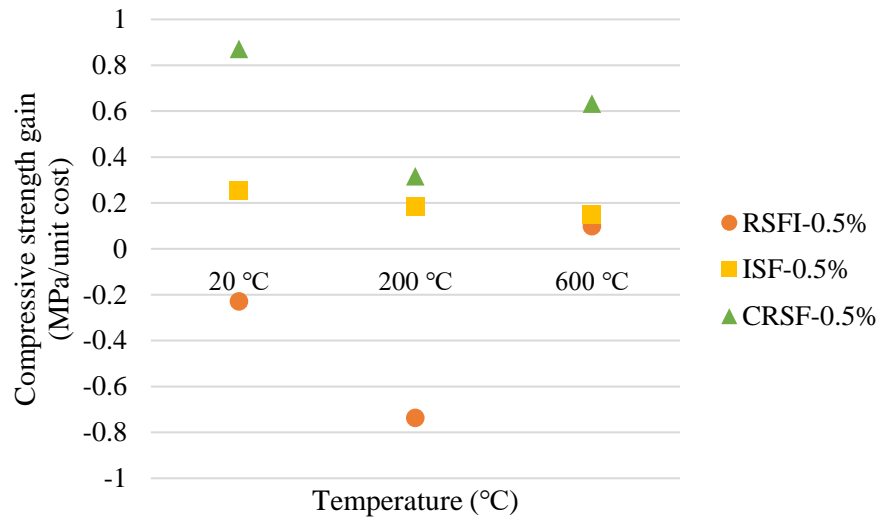


Fig. 19 (a) Compressive strength, (b) MOR gain per cost unit for mixtures at different temperatures

To maximize mechanical properties while lowering cost, CRSF can be used. ISF performs best in terms of mechanical properties, but these fibers have high costs. RSFI containing textiles and rubber showed the opposite trend; They were weaker in terms of mechanical performance but had less cost and a negative environmental impact. Among the concrete mix components, cement contributes the most to CO₂ emissions (Mastali et al., 2018a; Mastali et al., 2018b). The addition of fibers also leads to an increase in CO₂ emissions (Mastali et al., 2018a). However, industrial fibers' contribution to CO₂ emissions is higher than recycled fibers. According to the mechanical and economic analysis, CRSF can be a suitable alternative to ISF to strengthen concrete.

4. Conclusions

Considering the environmental and economic issues and the mechanical performance of concrete, this study has investigated the effect of RSF from waste tires at ambient and after exposure to high temperatures. The results obtained in summary are as follows:

- RSFI-0.5% specimens at ambient temperature and 200 °C did not improve compressive strength and had lower compressive strength than NC. The presence of rubber attached to the surface of fibers and textiles makes concrete compaction difficult, increases porosity, and thus decreases concrete strength. However, at 600 °C, it showed more residual strength than NC. This was while CRSF-0.5% caused a significant increase in compressive strength at all temperatures and presented similar behavior with ISF-0.5% at all temperatures.
- Fiber-reinforced concrete showed improved tensile strength and MOR at all temperatures. Bridging the cracks' fibers prevents the cracks' connection and propagation. At ambient temperature, RSFI-0.5% and CRSF-0.5% specimens slightly improved the tensile strength. The effect of recycled fibers is more significant at high temperatures. CRSF-0.5% specimens significantly improved the MOR at ambient and high temperatures, so their performance was better than ISF-0.5%.
- According to the mechanical and economic analysis, CRSF has shown results comparable to ISF at all temperatures; ISF is more expensive than CRSF. Therefore CRSF can be a suitable alternative to ISF to strengthen concrete.

References

- Aiello, M. A., Leuzzi, F., Centonze, G., & Maffezzoli, A. (2009). "Use of steel fibres recovered from waste tyres as reinforcement in concrete: Pull-out behaviour, compressive and flexural strength", *Waste management*, 29(6), 1960-1970. <https://doi.org/10.1016/j.wasman.2008.12.002>.
- Alsaif, A., Bernal, S. A., Guadagnini, M., & Pilakoutas, K. (2018). "Durability of steel fibre reinforced rubberised concrete exposed to chlorides", *Construction and Building Materials*, 188, 130-142.
- ASTM-C-1018-97. (1997). Standard Test Method for Flexural Toughness and First-Crack Strength of Fiber-Reinforced Concrete (Using Beam With Third-Point Loading).
- ASTM-C-1609.(2012) Standard Test Method for Flexural Performance of Fiber- Reinforced Concrete (Using Beam With Third-Point Loading).
- ASTM-C-39.(2018). Standard Test Method for Compressive Strength of Cylindrical Concrete Specimens. American Society for Testing and Materials, 100 Barr Harbor Drive, PO Box C700, West Conshohocken, PA 19428.
- ASTM-C494-13. (2015). Standard Specification for Chemical Admixtures for Concrete. Annu. B. ASTM Stand. Am. Soc. Test. Mater., 4.
- ASTM-C496-C496M-11. (2004). Standard test method for splitting tensile strength of cylindrical concrete specimens. West Conshohocken, PA: ASTM International.
- Awolusi, T. F., Oke, O. L., Atoyebi, O. D., Akinkurolere, O. O., & Sojobi, A. O. (2021). "Waste tires steel fiber in concrete: A review", *Innovative Infrastructure Solutions*, 6(1), 1-12. <https://doi.org/10.1007/s41062-020-00393-w>.
- Barros, J.A., Frazão, C., Caggiano, A., Folino, P., Martinelli, E., Xargay, H., Zamanzadeh, Z. and Lourenço, L. (2017). "Cementitious composites reinforced with recycled fibres", *Recent Advances on Green Concrete for Structural Purposes: The Contribution of the EU-FP7 Project EnCoRe*, 141-195. https://doi.org/10.1007/978-3-319-56797-6_8.
- Bedewi, N. (2009). "Steel fiber reinforced concrete made with fibers extracted from used tyres", *Master's thesis in Civil Engineering, Addis Ababa University, Addis Ababa, Ethiopia*.
- Behfarnia, K., & Behravan, A. (2014). "Application of high performance polypropylene fibers in concrete lining of water tunnels", *Materials & Design*, 55, 274-279. <https://doi.org/10.1016/j.matdes.2013.09.075>.
- Bezerra, A. C., Maciel, P. S., Corrêa, E. C., Soares Junior, P. R., Aguilar, M. T., & Cetlin, P. R. (2019). "Effect of high temperature on the mechanical properties of steel fiber-reinforced concrete", *Fibers*, 7(12), 100. <https://doi.org/10.3390/fib7120100>.
- Bulei, C., Todor, M. P., Heput, T., & Kiss, I. (2018). "Directions for material recovery of used tires and their use in the production of new products intended for the industry of civil construction and pavements", *In IOP Conference Series: Materials Science and Engineering*, 294, 012064. <https://doi.org/10.1088/1757-899X/294/1/012064>.
- Dehghanpour, H., & Yilmaz, K. (2018). "MECHANICAL AND IMPACT BEHAVIOR ON RECYCLED STEEL FIBER REINFORCED CEMENTITIOUS MORTARS", *Scientific Herald of the Voronezh State University of Architecture & Civil Engineering.*, 39(3), 67-84.
- Dixon, D.E., et al. Standard Practice for Selecting Proportions for Normal, Heavyweight, and Mass Concrete (ACI 211.1-91). (1991). American Concrete Institute Farmington Hills, MI, USA.

- Frazão, C. M. V. (2019). "Recycled steel fiber reinforced concrete for Structural elements subjected to chloride attack: mechanical and durability performance", *PhD Thesis, University of Minho*.
- Fu, C., Ye, H., Wang, K., Zhu, K., & He, C. (2019). "Evolution of mechanical properties of steel fiber-reinforced rubberized concrete (FR-RC)", *Composites Part B: Engineering*, 160, 158-166. <https://doi.org/10.1016/j.compositesb.2018.10.045>.
- Hager, I. (2014). "Colour change in heated concrete", *Fire Technology*, 50(4), 945-958. <https://doi.org/10.1007/s10694-012-0320-7>.
- Handoo, S. K., Agarwal, S., & Agarwal, S. K. (2002). "Physicochemical, mineralogical, and morphological characteristics of concrete exposed to elevated temperatures", *Cement and Concrete Research*, 32(7), 1009-1018. [https://doi.org/10.1016/S0008-8846\(01\)00736-0](https://doi.org/10.1016/S0008-8846(01)00736-0).
- Hossain, K. M. A., Lachemi, M., Sammour, M., & Sonebi, M. (2013). "Strength and fracture energy characteristics of self-consolidating concrete incorporating polyvinyl alcohol, steel and hybrid fibres", *Construction and Building Materials*, 45, 20-29. <https://doi.org/10.1016/j.conbuildmat.2013.03.054>.
- Jamshaid, H., & Mishra, R. (2016). "A green material from rock: basalt fiber—a review", *The Journal of The Textile Institute*, 107(7), 923-937. <https://doi.org/10.1080/00405000.2015.1071940>.
- Karimipour, A., Ghalehnovi, M., Edalati, M., & De Brito, J. (2021). "Properties of fibre-reinforced high-strength concrete with nano-silica and silica fume", *Applied Sciences*, 11(20), 9696. <https://doi.org/10.3390/app11209696>.
- Liew, K. M., & Akbar, A. (2020). "The recent progress of recycled steel fiber reinforced concrete", *Construction and Building Materials*, 232, 117232. <https://doi.org/10.1016/j.conbuildmat.2019.117232>.
- Ma, Q., Guo, R., Zhao, Z., Lin, Z., & He, K. (2015). "Mechanical properties of concrete at high temperature—A review", *Construction and Building Materials*, 93, 371-383. <https://doi.org/10.1016/j.conbuildmat.2015.05.131>.
- Mastali, M., Dalvand, A., Sattarifard, A. R., & Illikainen, M. (2018a). "Development of eco-efficient and cost-effective reinforced self-consolidation concretes with hybrid industrial/recycled steel fibers", *Construction and Building Materials*, 166, 214-226. <https://doi.org/10.1016/j.conbuildmat.2018.01.147>.
- Mastali, M., Dalvand, A., Sattarifard, A. R., Abdollahnejad, Z., & Illikainen, M. J. C. P. B. E. (2018b). "Characterization and optimization of hardened properties of self-consolidating concrete incorporating recycled steel, industrial steel, polypropylene and hybrid fibers", *Composites Part B: Engineering*, 151, 186-200. <https://doi.org/10.1016/j.compositesb.2018.06.021>.
- Memon, S. A., Shah, S. F. A., Khushnood, R. A., & Baloch, W. L. (2019). "Durability of sustainable concrete subjected to elevated temperature—A review", *Construction and Building Materials*, 199, 435-455. <https://doi.org/10.1016/j.conbuildmat.2018.12.040>.
- Modarres, Y., Ghalehnovi, M., (2022). "The effect of recycled steel fibers from waste tires on concrete properties", *Civil Engineering Infrastructures Journal*. doi: [10.22059/cej.2022.339592.1820](https://doi.org/10.22059/cej.2022.339592.1820)
- Mohajerani, A., Hui, S. Q., Mirzababaei, M., Arulrajah, A., Horpibulsuk, S., Abdul Kadir, A., ... & Maghool, F. (2019). "Amazing types, properties, and applications of fibres in construction materials", *Materials*, 12(16), 2513. <https://doi.org/10.3390/ma12162513>.

- Ramezani, A., Esfahani, M. (2018). "Evaluation of Hybrid Fiber Reinforced Concrete Exposed to Severe Environmental Conditions", *Civil Engineering Infrastructures Journal*, 51(1), 119-130. doi: [10.7508/cej.2018.01.007](https://doi.org/10.7508/cej.2018.01.007)
- Roesler, J. R., Altoubat, S. A., Lange, D. A., Rieder, K. A., & Ulreich, G. R. (2006). "Effect of synthetic fibers on structural behavior of concrete slabs-on-ground", *ACI materials journal*, 103(1), 3.
- Rosli, S., & Ibrahim, I. (2012). "Mechanical properties of recycled steel tire fibres in concrete", *Technical Report, Faculty of Civil Engineering, University Technology Malaysia*.
- Shannag, M. J. (2011). "Characteristics of lightweight concrete containing mineral admixtures", *Construction and Building Materials*, 25(2), 658-662. <https://doi.org/10.1016/j.conbuildmat.2010.07.025>.
- Tlemat, H., Pilakoutas, K., & Neocleous, K. (2006). "Stress-strain characteristic of SFRC using recycled fibres", *Materials and structures*, 39(3), 365-377. <https://doi.org/10.1007/s11527-005-9009-4>.
- Wang, Y., Wu, H. C., & Li, V. C. (2000). "Concrete reinforcement with recycled fibers", *Journal of materials in civil engineering*, 12(4), 314-319.
- Wu, H., Lin, X., & Zhou, A. (2020). "A review of mechanical properties of fibre reinforced concrete at elevated temperatures", *Cement and Concrete Research*, 135, 106117. <https://doi.org/10.1016/j.cemconres.2020.106117>.
- Xing, Z., Beaucour, A. L., Hebert, R., Noumowe, A., & Ledesert, B. (2015). "Aggregate's influence on thermophysical concrete properties at elevated temperature", *Construction and Building Materials*, 95, 18-28. <https://doi.org/10.1016/j.conbuildmat.2015.07.060>.
- Yang, J., Peng, G. F., Shui, G. S., & Zhang, G. (2019). "Mechanical properties and anti-spalling behavior of ultra-high performance concrete with recycled and industrial steel fibers", *Materials*, 12(5), 783. <https://doi.org/10.3390/ma12050783>.
- Zhang, P., Kang, L., Wang, J., Guo, J., Hu, S., & Ling, Y. (2020). "Mechanical properties and explosive spalling behavior of steel-fiber-reinforced concrete exposed to high temperature—a review", *Applied Sciences*, 10(7), 2324. <https://doi.org/10.3390/app10072324>.